

CHARACTERISTICS OF POLAR CUSP VLF EMISSIONS OBSERVED BY ISIS SATELLITES OF LOW ALTITUDE POLAR ORBIT

Tadanori ONDOH

Space Earth Environment Laboratory, 5186 Kitano, Tokorozawa 359

Abstract: Characteristics of polar cusp hiss and other VLF emissions observed in the cusp region are studied by using f - t spectra and narrow-band intensity data at six frequencies which were processed from VLF electric field data received from ISIS-1 and ISIS-2 at Syowa Station, Antarctica. The polar cusp hiss is very irregular in frequency, intensity and time (or space), and shows fine intensity variations in the narrow-band intensity data at 5 and 8 kHz bands as compared with coarse intensity variations of the polar hiss (or auroral hiss) appearing on either side of the polar cusp region. The polar cusp hiss occurs over several hours centered around the geomagnetic noon in geomagnetic local time for a few minutes in UT on ISIS west to east passes. The regions of polar hiss with curtain-like f - t spectrum lie on both sides of the polar cusp hiss region. The irregular and structured spectra of polar cusp hiss and saucer emissions may reflect irregular and structured electron precipitations in the cusp region. The polar cusp VLF emissions, such as the polar cusp hiss and VLF saucers occur at invariant latitudes from 72° to 86° , and at geomagnetic local times from 09 to 15 hours. The polar cusp VLF hiss is discussed in terms of the whistler-mode cherenkov radiations generated from downgoing electrons in the polar magnetosphere.

1. Introduction

Plasma waves in the polar cusp region at high altitudes were first observed by Hawkeye-1 of highly eccentric polar orbiter with apogee of $20.5 R_E$ (Earth's radius) launched on June 3, 1974 (GURNETT and FRANK, 1978). Their observational results are as follows; Only the ULF-ELF magnetic noise was uniquely associated with the polar cusp at invariant latitudes of 76° – 82° . Intense whistler-mode auroral hiss was observed in the polar cusp, over the polar cap and inside the nightside auroral zone. Near the earth, at $r < 2 R_E$, the auroral hiss was detected on nearly every pass through the polar cusp. However, they showed only frequency-time (f - t) spectra of plasma waves in compressed time scale.

Irregular f - t spectra of polar cusp hiss, which show fine intensity variations in narrow band intensity data, were first reported by ONDOH *et al.* (1981) on ISIS-2 west to east pass of July 11, 1977. ONDOH (1991a) obtained a polar map of the auroral hiss occurrence rate with a symmetric axis of 10–22 MLT (magnetic local time) meridian at invariant latitudes above 70° by removing irregular polar

cusp hiss from the ISIS VLF data, and he has proposed from the hiss occurrence map that the auroral hiss should be called as the polar hiss. KASAHARA *et al.* (1995) have shown a similar statistical result of the auroral hiss observed at altitudes between 3000 km and 5000 km by the Akebono satellite.

CARBARY and MENG (1986a) showed polar cusp signatures at low altitudes by using the 50 eV to 20 keV electron data observed by DMSP F2 and F4, and discussed relations between IMF- B_z , AE and cusp latitude. The polar cusp is recognized in the DMSP time profiles within a few minutes by enhanced electron fluxes exceeding $10^8/\text{cm}^2 \text{ s sr}$ and lowered average electron energies to below 200 eV. Such changes occur at both the poleward and equatorward boundaries on time scale of a few seconds in satellite time. The identified cusp signatures were generally restricted to the MLT range from 08 to 14 hours. Generally, the equatorward cusp boundary tends to change coherently with the IMF- B_z and AE . But, during magnetically quiet times, the cusp boundary exhibits considerable variability that is not associated with variations in IMF- B_z or AE , and the cusp location varies randomly between invariant latitudes of 75° and 80° . The time integral of southward IMF- B_z exerts a dominant influence on the latitude at the cusp equatorward boundary.

In this paper, we discuss detailed structures of polar cusp hiss by using high time resolution ISIS f - t spectra received at Syowa Station, Antarctica and show statistical distributions of the polar cusp VLF emissions in invariant latitude and in geomagnetic local time. Then, we discuss the generation mechanism of polar cusp hiss.

2. Characteristics of Polar Cusp VLF Emissions Observed in Topside Ionosphere

Figure 1 shows narrow-band intensity data at six frequency bands (300 Hz, 1.5, 5, 8, 16 and 20 kHz) received from ISIS-1 on April 12, 1978 ($K_p = 3-$) at Syowa Station (geomagnetic latitude 69.7°S , longitude 77.7°E), Antarctica. The narrow-band intensity data are processed from ISIS VLF wide-band electric field data (50 Hz–30 kHz) by narrow-band filter banks and detectors with a minimum reading circuit of charging and discharging time constant of 10 s and 10 ms, respectively. The dynamic range of the narrow-band intensity data is about 30 dB in arbitrary scale, while that of the f - t spectra is about 10 dB. Figure 1 shows fine intensity variations for 3 min from 1414 UT (Invariant latitude 76.4° , 1338 MLT) to 1417 UT (77.0° , 1034 MLT) between two upward arrows as compared with enhanced intensity variations outside the arrows. The fine intensity variations are due to the spatial variations in longitude because the geomagnetic local time changed widely from the afternoon side to the morning side for only 3 min of time. The enhanced coarse intensity variations outside the upward arrows are produced by a stable polar hiss (or auroral hiss) of curtain-like spectrum with a lower limit frequency of the lower hybrid resonant (LHR) frequency as shown by Figs. 2a–2b. In Fig. 1, broadband polar hiss appearing at frequencies above 5 kHz occurs at invariant latitudes above 66° and ELF hiss (300 Hz) does at latitudes below about 73° .

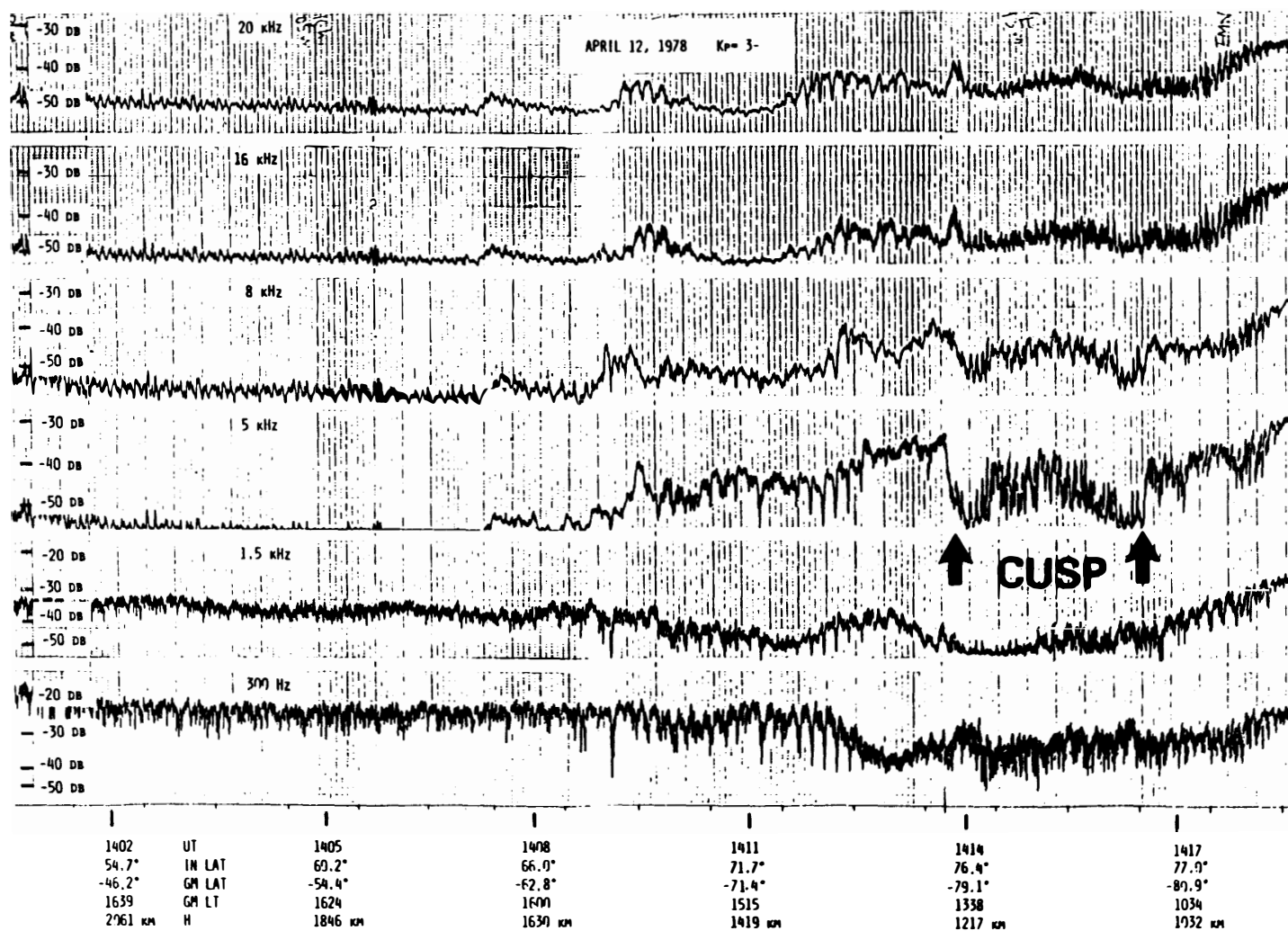


Fig. 1. Fine intensity variations of irregular polar cusp hiss at 5 and 8 kHz bands between two arrows observed by ISIS-1 on April 12, 1978, $K_p=3-$.

Figures 2a–2b show f - t spectra of polar cusp hiss corresponding to the fine intensity variations between the two arrows in Fig. 1. The linear frequency scale is from dc to 10 kHz and the linear time scale is 30 s from the left end to the right end in all panels in Figs. 2a–2b. The top panel of Fig. 2a illustrates a stable polar hiss (or auroral hiss) of curtain-like spectrum at 1413:40 UT and invariant latitude 76.0° . However, all panels from the upper second one at 1414:20 UT in Fig. 2a to the lower one at 1416:30 UT in Fig. 2b show irregular spectra of polar cusp hiss in time or space, intensity and frequency. The irregular spectra of polar cusp hiss in Figs. 2a–2b corresponds well to the fine intensity variations at 5 and 8 kHz bands between the two arrows in Fig. 1. The latter half of the bottom panel in Fig. 2b shows again a stable curtain-like polar hiss at frequencies above 3 kHz. Consequently, the ISIS-1

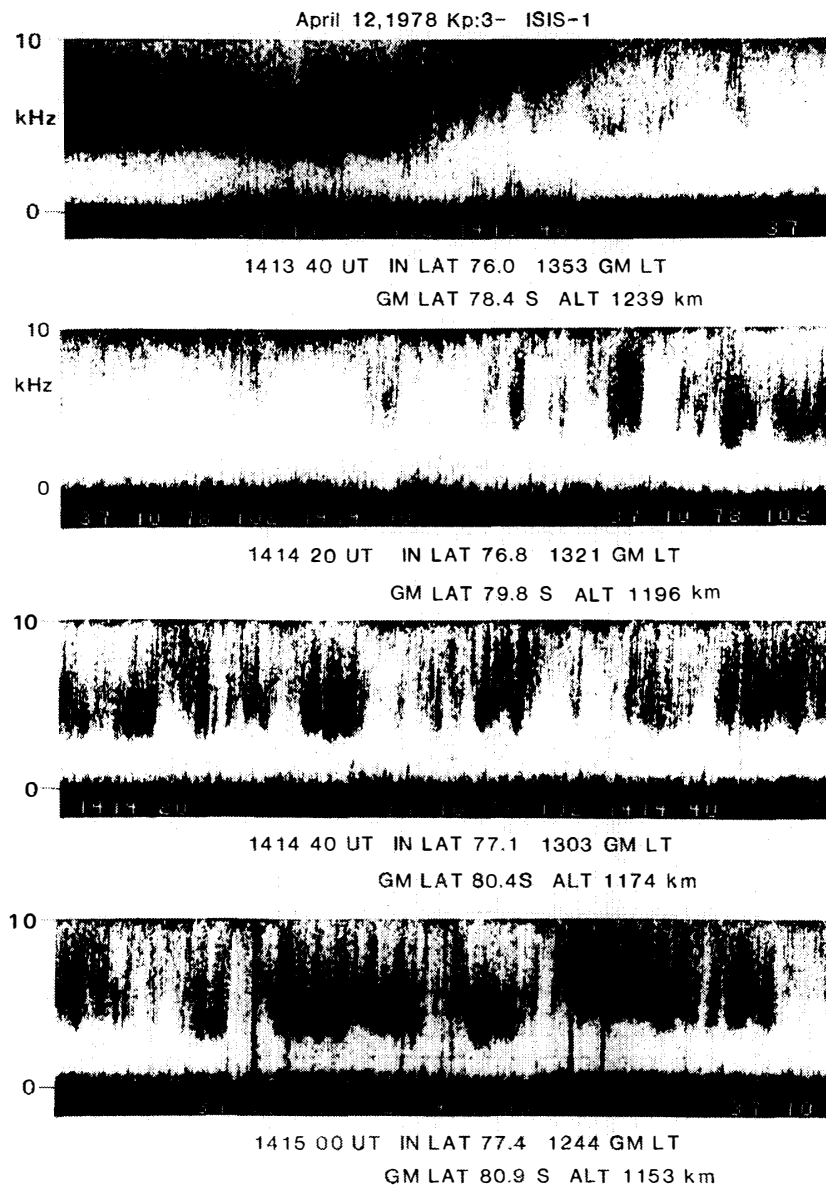


Fig. 2a.

seems to have left from the polar cusp region at 1417 UT (inv. lat. 77.0° , 1034 MLT). In this case, the ISIS-1 moved in the west-east direction along a circle of geomagnetic latitude around 80° (inv. lat. 76.5°). Thus, the ISIS-1 or ISIS-2 often observed irregular polar cusp hiss for a few minutes in UT at invariant latitudes from 74° to 84° and in geomagnetic local times from 9 to 14 hours.

Figure 3 shows a polar map of the occurrence rate of polar hiss for geomagnetic activities of $K_p=0-7$ obtained by removing the irregular polar cusp hiss from 347 ISIS VLF passes received at Syowa Station, Antarctica from June 1976 to January 1983, where occurrence rate contours of 0.3, 0.4 and 0.5 are illustrated

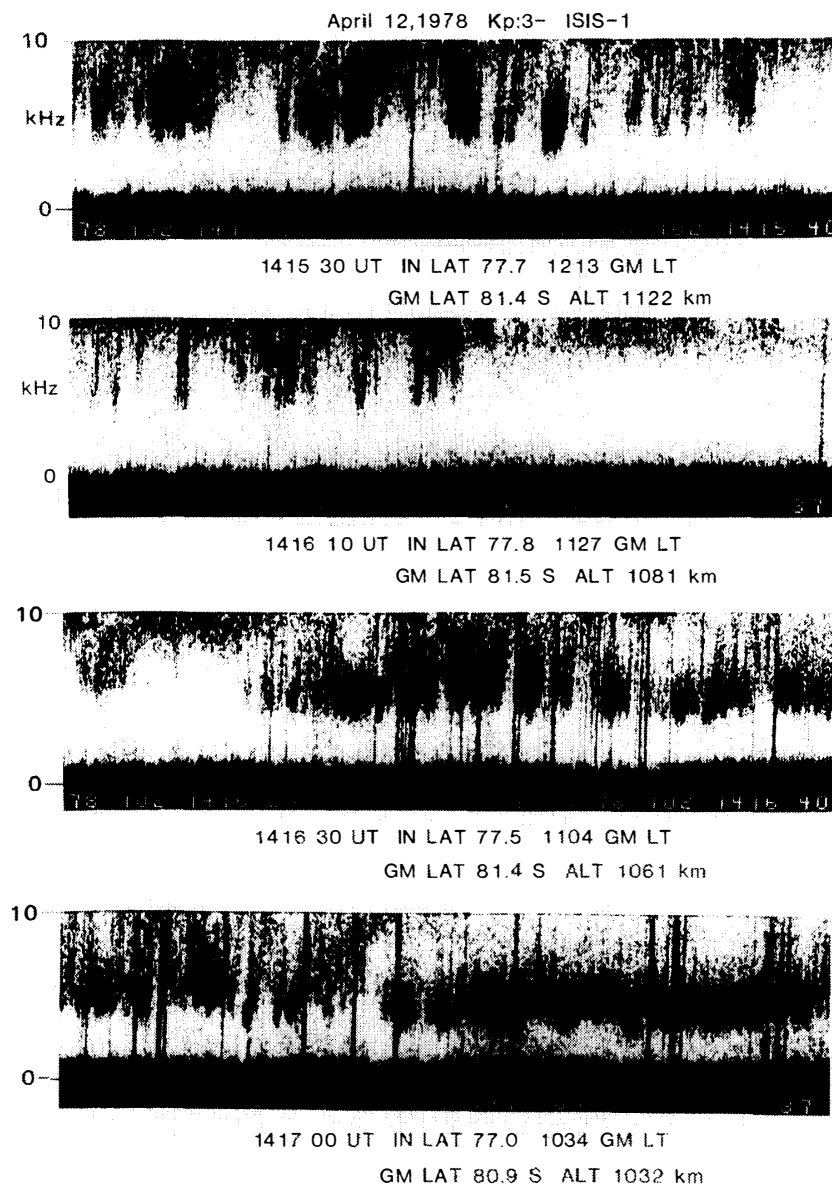


Fig. 2b.

Figs. 2a-b. Frequency-time spectra of irregular polar cusp hiss observed by ISIS-1 on April 12, 1978. Top panel in Fig. 2a and bottom panel in Fig. 2b show stable curtain-like polar hiss (or auroral hiss), respectively.

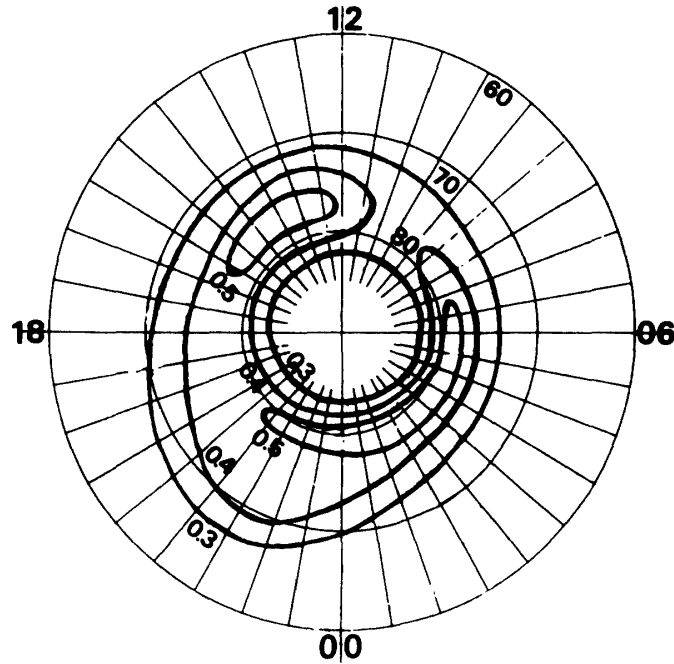


Fig. 3. Polar map of the occurrence rate for polar hiss obtained from 347 ISIS VLF paths ($K_p=0-7$) in invariant latitude and geomagnetic local time. Contours show occurrence rate of polar hiss.

(ONDOH, 1988). In Fig. 3, a low occurrence rate region is seen at local times around 10 MLT between invariant latitudes of 74° and 82° . This is a region of irregular polar cusp hiss lying between the high occurrence rate regions of stable curtain-like polar hiss (or auroral hiss) as shown by Figs. 1 and 2.

Figures 4a-4b show $f-t$ spectra of polar cusp VLF emissions observed on July 17, 1977 ($K_p=1+$) on ISIS-2 north-south pass from 1535:40 UT (inv. lat. 74.3° , 1145 MLT) to 1538:50 UT (inv. lat. 82.9° , 1234 MLT). The time and frequency scales in Figs. 4a-4b are the same as those in Figs. 2a-2b. The upper two panels of Fig. 4a show ELF hiss at frequencies below 2 kHz and VLF saucer emissions found often near the midnight (22-01 MLT) by ISIS satellites (ONDOH *et al.*, 1981; YOSHINO *et al.*, 1981). The occurrence rate of ELF hiss of which $f-t$ spectrum is similar to the plasmaspheric hiss decreases with increasing L beyond $L=4$ in the topside ionosphere (ONDOH *et al.*, 1983). The ELF hiss often extends to the auroral zone, and a local time variation for the highest geomagnetic latitude of ELF hiss occurrence follows approximately the auroral zone (ONDOH, 1991b). The right half of upper second panel in Fig. 4a indicates that the ISIS-2 entered into an irregular plasma wave region, that is, the polar cusp region at invariant latitude around 76° (1536:10 UT). Lower two panels in Fig. 4a show a lion-roar emission around 1 kHz (1536:40 UT) and polar cusp hiss with irregular lower limit frequency. Upper three panels in Fig. 4b show occurrences of VLF saucer emissions in the dayside polar cusp region. Since VLF saucer emissions are electrostatic waves generated by downgoing or upgoing electrons relatively near above or below the satellite (ONDOH *et al.*, 1984), the occurrence of VLF saucer emissions implies that low energy

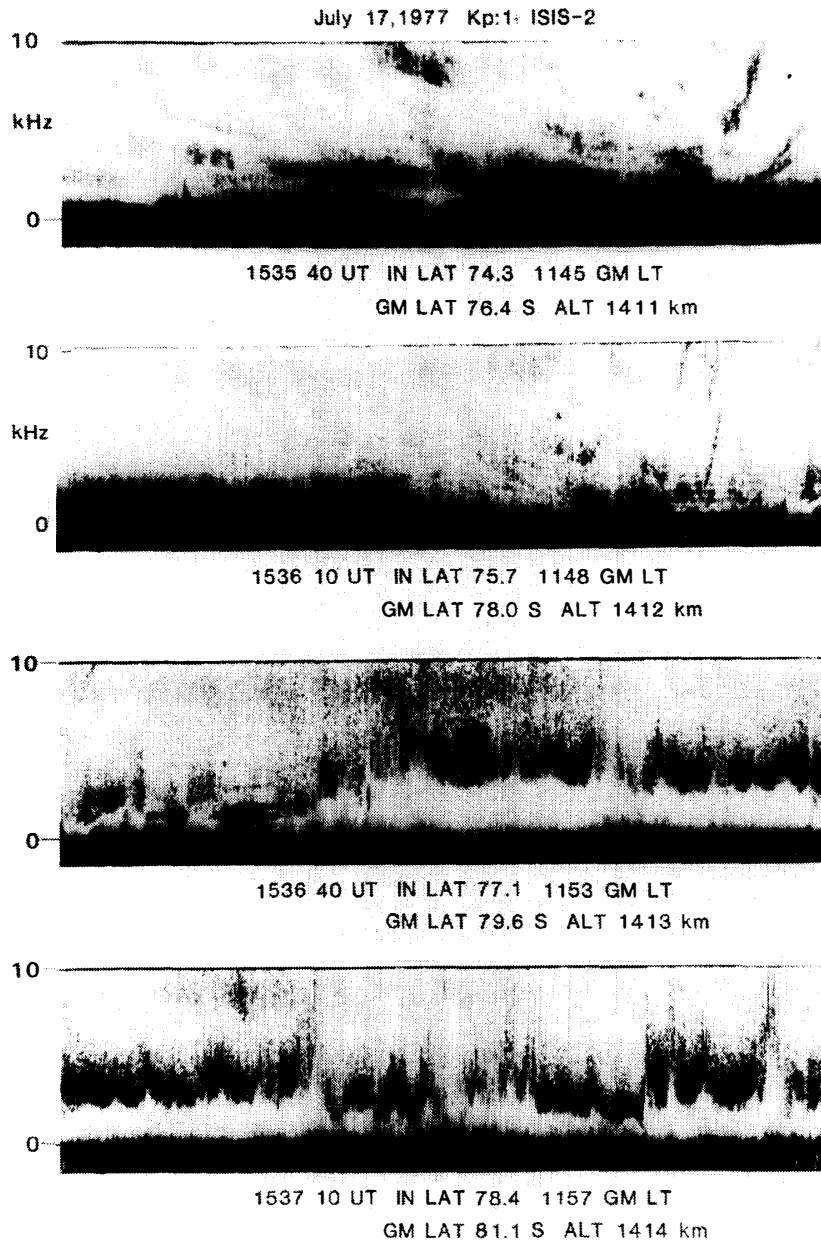


Fig. 4a.

electrons precipitate into the polar cusp region. The bottom panel in Fig. 4b shows a stable curtain-like polar hiss at frequencies above 2 kHz. This means that the ISIS-2 left the polar cusp region around 1539 UT at invariant latitude around 83° (1234 UT). Figure 5 is narrow-band intensity ISIS VLF data including the period of Figs. 4a-4b (July 17, 1977). The polar cusp region discussed by $f-t$ spectra of Figs. 4a-4b may be shown by two upward arrows in Fig. 5, but it is not clear because strong signals of the polar cusp hiss lie between 1.5 kHz and 5 kHz. In Fig. 5, the ISIS-2 crossed a border between the noon and midnight sides over the polar cap at 1541 UT, when an intense broad-band polar hiss was suddenly observed at 5, 8, 16 and 20 kHz bands. Large fine intensity variations at 5, 8, 16 and 20 kHz bands and intense

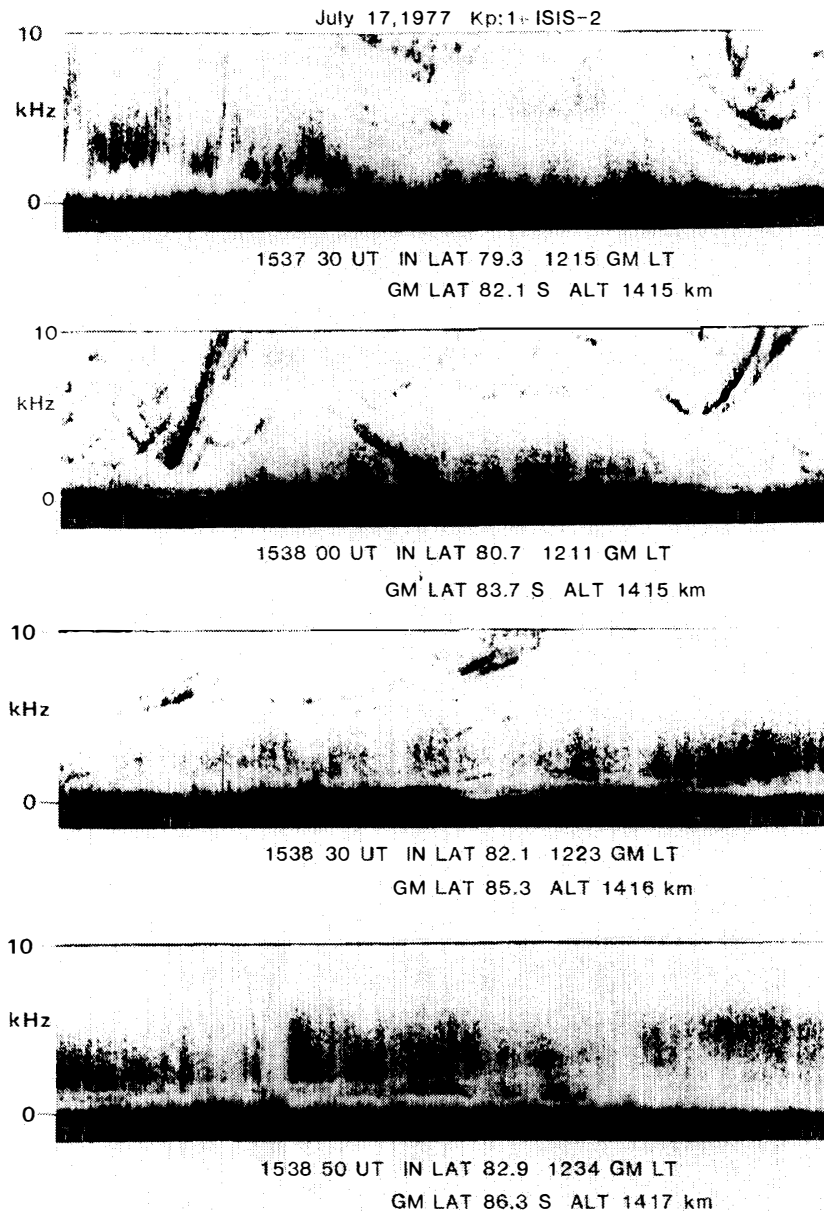


Fig. 4b.

Figs. 4a-b. Frequency-time spectra of polar cusp VLF emissions, such as VLF saucers and irregular polar cusp hiss observed by ISIS-2 on July 17, 1977, $K_p=1+$. Top panel in Fig. 4a and bottom panel in Fig. 4b show ELF hiss at frequencies below 2 kHz and stable polar hiss, respectively.

stable ELF hiss at 300 Hz band are seen on the noon side, while a relatively coarse intensity variations of the stable broad-band polar hiss at 5, 8, 16 and 20 kHz bands and relatively weak intensity variations at 300 Hz band are seen on the nightside. The intense stable polar hiss was observed over a wide polar cap region from above 84° to below 78° in invariant latitude. In this sense, the term "the auroral hiss" should be replaced by "the polar hiss" as proposed by ONDOH (1991a).

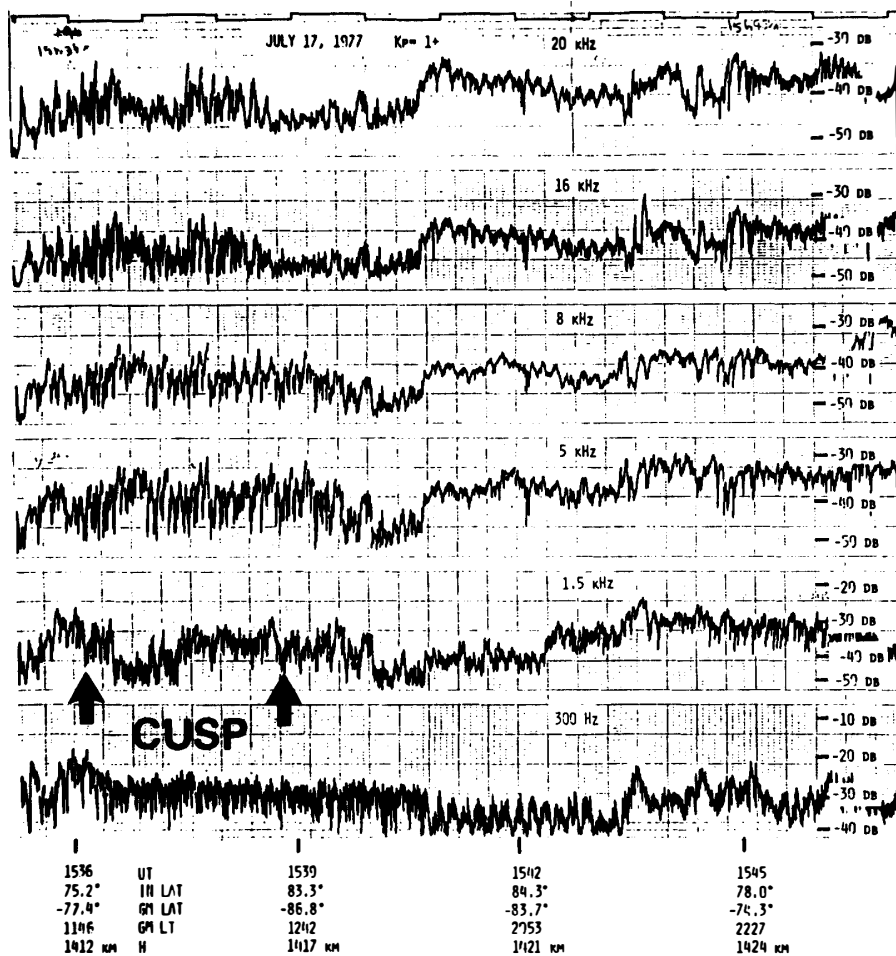


Fig. 5. Narrow-band intensity data processed from ISIS-2 VLF data tape of July 17, 1977. A period between two arrows indicates the interval of f - t spectra of polar cusp VLF emissions in Figs. 4a-4b.

Next, we have selected 76 ISIS VLF paths with polar cusp VLF emissions, such as Figs. 2 and 4 from 108 ISIS-1 and ISIS-2 paths received during June 1976 to August 1978 at Syowa Station, Antarctica. Upper and lower panels in Fig. 6 show invariant latitude and geomagnetic local time dependence of the occurrence rate for polar cusp VLF emissions statistically obtained from 76 ISIS VLF paths for geomagnetic activities of $K_p=1-4$, respectively. The polar cusp VLF emissions occur mainly between invariant latitudes of 74° and 84° , and between geomagnetic local times of 9 and 15 hours. High occurrence rates of the polar cusp VLF emissions lie at invariant latitudes from 76° to 80° and at geomagnetic local times from 11 to 13 hours. According to statistical studies of particle observations by polar orbiting satellites (KREMSER and LUNDIN, 1990; NEWELL and MENG, 1988), the polar cusp is the main particle entry region centered around local noon and latitude of about 80° . CARBARY and MENG (1986b) obtained a statistical distribution of polar cusp signatures for precipitating low energy electrons measured by two circular orbiters, DMSP F2 and F4 with altitude of 840 km. The polar cusp signatures occur between 10 and 16 hours in MLT and between 67° and 82° in

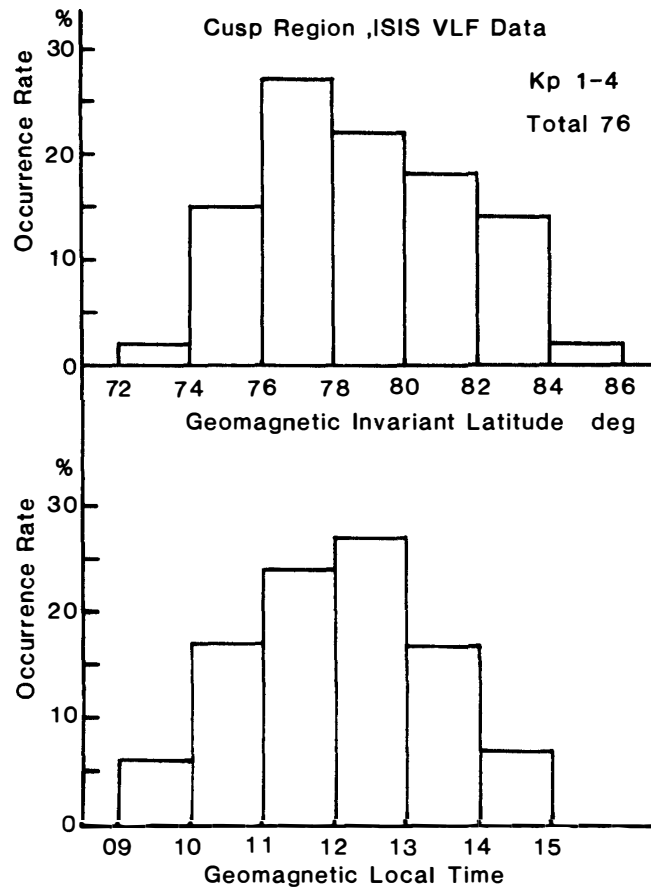


Fig. 6. Distributions of polar cusp VLF emissions, such as polar cusp hiss and VLF saucer emissions in geomagnetic invariant latitude (upper half) and in geomagnetic local time (lower half). These VLF data of 76 ISIS paths were observed from June 1976 to August 1978.

invariant latitude. These results on the polar cusp region are similar to those for the high occurrence rate region of polar cusp VLF emissions observed by ISIS satellites (Fig. 6) in latitude and local time. Therefore, the polar cusp VLF emissions seem to be generated by precipitating low energy electrons into the polar cusp region.

3. Discussions on Generation of Polar Cusp Hiss

Irregular f - t spectra and fine intensity variations of the polar cusp hiss as shown in Figs. 1 and 2 are transient phenomena, and they may be generated by highly structured low energy electrons, such as the polar squall (WINNINGHAM and HEIKKILA, 1974). The frequency range of polar cusp hiss may reflect the energy range of precipitating electrons, and the intensity time variation may represent mainly the spatial or longitudinal dependence of electron precipitations since the polar cusp hiss is normally observed over several hours in MLT for a few minutes on ISIS west to east paths. GURNETT and FRANK (1978) observed intense whistler mode auroral hiss in the polar cusp, over the polar cap and in the nightside auroral zone by Hawkeye-1, but they did not find any fine structures of the cusp auroral hiss

(or polar cusp hiss) in f - t spectra with compressed time scale. ONDOH (1990) has shown that the broad-band auroral hiss (or polar hiss) is explained by the whistler mode cherenkov radiations generated from downgoing inverted V electrons with energy of 50 eV–40 keV in the polar magnetosphere. KASAHARA *et al.* (1995) showed that the V-shaped auroral hiss comes down to the spacecraft in the polar magnetosphere according to the Akebono observations.

The whistler-mode cherenkov radiation from downcoming electrons with wide energy range is a powerful generation mechanism to explain wide band noises like the hiss. The frequency of whistler mode cherenkov radiations is given by $f = Ef_p^2 \cos \theta / 250 f_H$ kHz, where θ is the wave normal angle to the geomagnetic field line, f_H the electron gyrofrequency, f_p the electron plasma frequency and $E = 250 (V/c)^2$ keV for the parallel electron velocity, V . From this expression, we have the upper limit frequency of whistler-mode cherenkov radiation given by $f \leq Ef_p^2 / 250 f_H$ kHz. Qualitatively, low frequency components of the whistler mode cherenkov radiation are generated at relatively higher altitudes, and the high frequency components are generated at relatively lower altitudes on the same field line. In fact, the frequency and intensity of occurrence of the whistler mode auroral hiss observed by Hawkeye-1 generally increase with decreasing altitude (GURNETT and FRANK, 1978). Figure 7 shows altitude profiles for the frequency of whistler mode cherenkov radiations generated from precipitating electrons with energy of 5 and 30 keV along a geomagnetic field line of invariant latitude 77° in the model polar magnetosphere computed by $f = Ef_p^2 / 250 f_H$ (ONDOH, 1991a; PERSOON *et al.*, 1983). In Fig. 7, the 5 and 30 keV electrons generate, respectively, 2 kHz waves of whistler mode cherenkov radiations at altitudes around 3300 and 5900 km, and also the 30 keV electrons generate 5 kHz waves around 4100 km in the polar magnetosphere. These calculated results in Fig. 7 depend strongly on the model distributions of electron density, geomagnetic field and energy of precipitating electrons. Thus, the polar cusp hiss appearing at frequencies above 2 kHz as observed by ISIS satellites seems to be generated by downcoming electrons with energy above a few keV at relatively low altitudes in the polar magnetosphere. Therefore, the auroral VLF hiss observed at high altitudes by Hawkeye-1 appears to propagate upward away from low altitude sources as suggested by GURNETT and FRANK (1978).

However, low altitude satellite observations show good correspondences between large fluxes of low energy electrons around 100 eV and the auroral hiss in the polar cusp (GURNETT and FRANK, 1972; LAASPERE and HOFFMAN, 1976), and a good cusp signatures involving the increase of low energy electron flux exceeding $10^8/\text{cm}^2 \text{ s sr}$ and the lowering of the electron average energy to below about 200 eV (CARBARY and MENG, 1986b). Low energy electrons with energy below 200 eV can generate only whistler-mode cherenkov radiations below ELF band in the polar magnetosphere as deduced from the expression of $f \leq Ef_p^2 / 250 f_H$. The lower limit electron energy for generating the whistler-mode cherenkov radiation is given by $E \geq 250 f_H^2 / f_p^2$. This expression suggests that the whistler-mode cherenkov radiation in VLF range might be generated by low-energy electrons below 1 keV, if a local electron density is sufficiently high in the polar magnetosphere. An uncertainty

range of the electron density in the nightside polar magnetosphere is as high as $\pm 40\%$ (PERSOON *et al.*, 1983). So, for maximum electron densities of $2660/\text{cm}^3$, $42/\text{cm}^3$, and $7/\text{cm}^3$ at geocentric distance of 1.32, 2.0 and $3.0 R_E$ on a geomagnetic field line of invariant latitude 77° , the lower limit electron energies for generating the whistler-mode cherenkov radiations at 5 kHz are estimated at 4, 80 and 135 keV, respectively by the above expression. Thus, some acceleration of the low energy electrons at altitudes above the ISIS orbits is required for generating VLF whistler-mode cherenkov radiations in the magnetospheric polar cusp region. Further satellite observations of particles and plasma waves at middle altitudes in the polar magnetosphere are necessary for understanding the relation between polar cusp hiss and precipitating particles in the vicinity of the polar cusp.

4. Conclusion

VLF electric field data (50 Hz–30 kHz) received from ISIS-1 and ISIS-2 at Syowa Station, Antarctica are analyzed by using frequency-time spectra and narrow-band intensity data at six frequency bands. Irregular f - t spectra of the polar cusp hiss appearing at frequencies above 2 kHz were observed over several hours in MLT for a few minutes in UT on ISIS west to east pass on April 12, 1978. These spectra show spatial variations of the polar cusp hiss. Outside both sides of the irregular spectrum region, there are regions of the stable curtain-like spectra for the polar hiss (or auroral hiss). The corresponding narrow-band intensity data at 5 and 8 kHz bands show fine time variations of the polar cusp hiss intensity over several hours in MLT, while, on the both sides of the polar cusp hiss region, there are regions of slow intensity variations for the stable curtain-like polar hiss. Also, a region of polar cusp VLF emissions, such as VLF saucer emissions and irregular polar cusp hiss was found between two regions of the stable polar hiss on other ISIS paths.

Of 108 ISIS-1 and ISIS-2 paths received at Syowa Station from June 1976 to August 1978, 76 VLF paths showed the polar cusp hiss and VLF saucer emissions. Statistical result of these data shows that the polar cusp VLF emissions occur

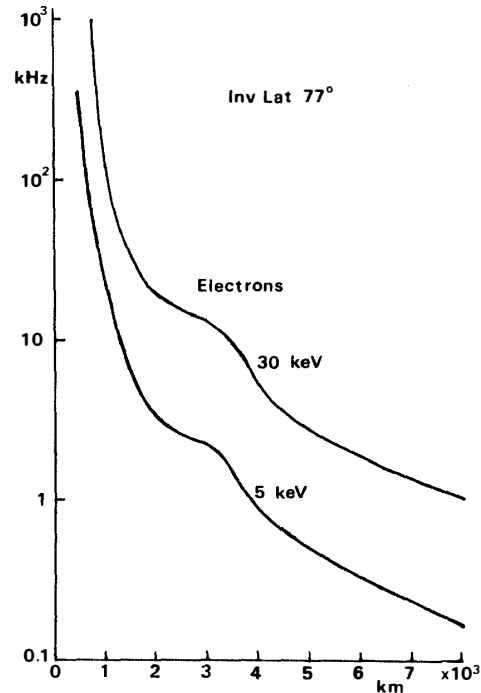


Fig. 7. Calculated altitude profiles of whistler mode cherenkov radiation frequency generated from downward electrons with energy of 5 and 30 keV along geomagnetic field line of invariant latitude 77° . The longitudinal axis and abscissa are shown in the logarithmic frequency scale and linear altitude scale, respectively.

between invariant latitudes of 72° and 86° , and between geomagnetic local times of 9 and 15 hours. The high occurrence rate region of polar cusp VLF emissions lies at invariant latitudes from 76° to 80° , and at geomagnetic local times from 11 to 13 hours. This result agrees well with the polar cusp region obtained from low energy electron observations by low altitude satellites.

However, it is difficult to explain the polar cusp hiss by the whistler-mode cherenkov radiation because low energy electrons with energy below 1 keV can not generate VLF whistler-mode cherenkov radiations for plasma parameters previously observed in the polar magnetosphere. Further satellite observations of precipitating electrons and plasma parameters in the polar cusp region are necessary for elucidating the generation of polar cusp hiss.

Acknowledgments

I would like to thank the wintering party members at Syowa Station, Antarctica for their collaboration in the data acquisition from the ISIS satellites.

References

- CARBARY, J. F. and MENG, C.-I. (1986a): Relations between the interplanetary magnetic field B_z , AE index, and cusp latitude. *J. Geophys. Res.*, **91**, 1549–1556.
- CARBARY, J. F. and MENG, C.-I. (1986b): Correlation of cusp latitude with B_z and AE (12) using nearly one year's data. *J. Geophys. Res.*, **91**, 10047–10054.
- GURNETT, D. A. and FRANK, L. A. (1972): VLF hiss and related plasma observations in the polar magnetosphere. *J. Geophys. Res.*, **77**, 172–190.
- GURNETT, D. A. and FRANK, L. A. (1978): Plasma waves in the polar observations from Hawkeye 1. *J. Geophys. Res.*, **83**, 1447–1462.
- KASAHARA, Y., YOSHIDA, K., MATSUO, T., KIMURA, I. and MUKAI, T. (1995): Propagation characteristics of auroral hiss observed by Akebono satellite. *J. Geomagn. Geoelectr.*, **47**, 509–525.
- KREMSEK, G. and LUNDIN, R. (1990): Average spatial distributions of energetic particles in the mid altitude cusp/cleft region observed by Viking. *J. Geophys. Res.*, **95**, 5753–5766.
- LAASPERE, T. and HOFFMAN, R. A. (1976): New results on the correlation between low-energy electrons and auroral hiss. *J. Geophys. Res.*, **81**, 524–530.
- NEWELL, P. T. and MENG, C.-I. (1988): The cusp and the cleft/boundary layer: Low-altitude identification and statistical local time variation. *J. Geophys. Res.*, **93**, 14549–14556.
- ONDOH, T. (1988): Occurrence map of broad-band auroral VLF hiss observed by ISIS satellites. *Proc. NIPR Symp. Upper Atmos. Phys.*, **1**, 153–167.
- ONDOH, T. (1990): Broad-band auroral VLF hiss and inverted-V electron precipitation in the polar magnetosphere. *J. Atmos. Terr. Phys.*, **52**, 385–397.
- ONDOH, T. (1991a): Polar hiss observed by ISIS satellites. *Magnetospheric Substorms*, ed. by J. R. KAN *et al.* Washington, D. C., Am. Geophys. Union, 387–398 (Geophysical Monograph 64).
- ONDOH, T. (1991b): Polar VLF emissions observed by ISIS satellites. *Environmental and Space Electromagnetics*, ed. by H. KIKUCHI. Berlin, Springer, 139–154.
- ONDOH, T., NAKAMURA, Y. and MURAKAMI, T. (1981): Characteristics of VLF saucers and auroral hiss from ISIS satellites received at Syowa Station, Antarctica. *Mem. Natl Inst. Polar Res.*, Spec. Issue, **18**, 54–71.
- ONDOH, T., NAKAMURA, Y., WATANABE, S., AIKYO, K. and MURAKAMI, T. (1983): Plasmaspheric hiss observed in the topside ionosphere at mid- and low-latitudes. *Planet. Space Sci.*, **31**,

411–422.

- ONDOH, T., WATANABE, S. and NAKAMURA, Y. (1984): VLF emissions observed by ISIS satellites during the IMS. Proc. Conf. Achievements of the IMS, ESA SP-217, 525–528.
- PERSOON, A. M., GURNETT, D. A. and SHAWHAN, S. D. (1983): Polar cap electron densities from DE-1 plasma wave observations. J. Geophys. Res., **88**, 10123–10136.
- WINNINGHAM, J. D. and HEIKKILA, W. J. (1974): Polar cap auroral electron fluxes observed with ISIS-1. J. Geophys. Res., **79**, 949–957.
- WOCH, J. and LUNDIN, R. (1992): Magnetosheath plasma precipitation in the polar cusp and its control by the interplanetary magnetic field. J. Geophys. Res., **97**, 1421–1430.
- YOSHINO, T., OZAKI, T. and FUKUNISHI, H. (1981): Occurrence distribution of hiss and saucer emissions over the southern polar region. J. Geophys. Res., **86**, 846–852.

(Received March 25, 1996; Revised manuscript accepted September 6, 1996)